OPTIMIZATION OF A FIRING FURNACE

B. R. Olaisen, A. Holt and E. S. Marstein
Section for Renewable Energy, Institute for Energy Technology
P.O. Box 40, NO-2027 Kjeller, Norway
email: birger.retterstol.olaisen@ife.no

ABSTRACT: This paper presents work on optimizing an RTC LA-309 firing furnace with four heat zones and water cooling. The belt speed and temperature setpoints in the different heat zones were used to vary the firing temperature profile, while air and water flows were held constant. It was found that the best results were achieved at a belt speed of 250 cm/min with a peak temperature on the wafer between 785°C and 830°C, and a time above 620°C between 11.6 seconds and 12.7 seconds. Solar cells of up to 15.5% efficiency and a fill factor up to 78% were fired at these parameters. Low temperatures combined with high belt speeds were found to give incomplete firing, while high temperature and slow belt speed gave high contact resistance at the interface between silicon and the contacts.

Keywords: Contacts, Screen-printing, Multi-crystalline silicon

1 INTRODUCTION

Peak electrical performance of the solar cells is necessary to reach high efficiencies in production, but also in a a research laboratory, a stable and good metallization process is of utmost importance. Even moderate values of series resistance or shunt resistance would result in low efficiencies and fill factors for all samples, and thus masking a possible positive effect of an altered process step. Therefore, having an optimized firing process is important in solar cell research, both concerning the best achievable results, and the width of the process window.

Our research institute has recently bought a new RTC LA-309 firing furnace with four heat zones and water cooling in addition to the normal forced air flow cooling. In this work, different temperature profiles have been systematically examined to find the optimum firing condition for this furnace. In order to alter the temperature profile, the belt speed and setpoint temperatures in the four heat zones were varied, while the air and water flows were held constant.

The IV curves from all samples in this work were analyzed with the computer program IVFIT [1] to extract the characteristic parameters, and selected samples were mapped with Corescan [2] to examine the cause of the measured series resistance.

2 EXPERIMENTAL

The RTC LA-309 firing furnace used in this work had four heat zones and both water cooling and forced air flow cooling. The rated maximum temperature for each heat zone was 1050°C, and the furnace was capable of belt speeds up to 700 cm/min. Each heat zone was 7.5 inches long, which gives a total length for all four heat zones of approximately 76 cm.

For simplicity, the setpoint temperature was increased linearly from heat zone to heat zone, and the first heat zone was always set to 780°C. The temperature setpoints in the four heat zones defines a setpoint profile, such as 780-830-880-930. In this work, the setpoint profile can thereby be uniquely identified by the setpoint temperature in the last heat zone, which also is the maximum setpoint temperature. The maximum setpoint temperature was varied between 795°C and 1020°C.

Belt speeds between 200 cm/min and 300 cm/min were used in this work, which give a total time in the heat zones between 15 seconds and 25 seconds. The belt speed combined with the setpoint profile defines one set of parameters used to fire solar cells in this work.

The temperature of 780°C was rather arbitrarly selected as temperature in the first heat zone because earlier setpoint profiles prior to this work used this temperature. The air flow in the heating chamber was set to 70 SCFH, while the other flow meters were set to 1/3 of the rated maximum for each flow meter. The water flow was about 18 litre per minute, and the temperature of the water typically rose by 2°C inside the furnace.

For each given set of parameters, a temperature profile was measured by placing a thermocouple in contact with a test wafer, and sending the assembly through the furnace. To be able to measure rapid temperature variations without disturbing the measurement, the thermocouple had a wire diameter of only 0.5 mm.

The samples used for the optimization were 125 mm square multicrystalline silicon solar cells, and both the emitter and the SiN antireflection layer were of good uniformity. REC Scancell AS did most of the cell processing, while the contact formation were done at the Institute for Energy Technology (IFE). The emitters were made by $POCl_3$ diffusion, and had a sheet resistance of 50 Ω/☐. Edge isolation was done by dry etching in a plasma chamber, and the SiN layers were deposited by PECVD. Contacts were screen-printed onto the samples by a conventional screen-printer. The pastes used were Du Pont PV147 for the front grid, Du Pont PV202 for the back busbars, and Ferro FX53-038 for the aluminum back contact.

At least 3 samples were fired at each set of parameters. To clearify the results, a total of 6 out of 147 samples were excluded from the final dataset. These samples deviated from the other samples fired at the same parameters by more than 4% absolute in efficiency. They were eliminated because the performance was not determined by the firing process, but due to broken or partly broken fingers, edge shunting or other non-firing related defects.

3 RESULTS AND DISCUSSION

3.1 Temperature profiles

The measured temperature profiles depended both on the belt speed and the setpoint profile. Figure 1 shows an example where the belt speed was altered while the

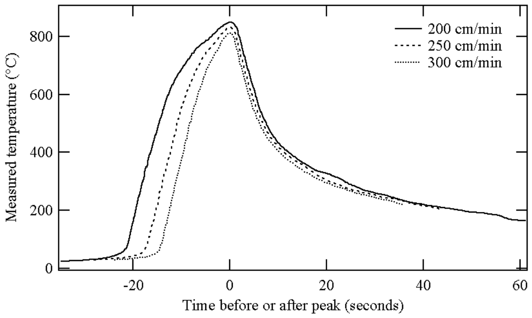

Figure 1: Measured temperature profiles of a setpoint profile of 780-830-880-930 at different belt speeds.

setpoint profile was constant. As expected, higher belt speeds gave lower peak temperature. To reach the same peak temperature when the belt speed was altered, the setpoint temperatures must also had to be changed. Table 1 shows some characteristic measurements from the temperature profiles shown in figure 1.

Belt speed (cm/min)	Heating rate	Cooling rate	Peak temp	Time above 620°C
200	62°C/s	62°C/s	810°C	17.1 s
250	65°C/s	65°C/s	830°C	12.7 s
300	69°C/s	65°C/s	850°C	9.6 s

Table 1: The heating rate between 100°C and 600°C, the cooling rate between 775°C and 625°C, the peak temperature, and the time above 620°C for the temperature profiles shown in figure 1.

For each belt speed, figure 2 shows a plot of the measured peak temperature at different maximum setpoint temperatures. The peak temperature varied roughly linearly with the maximum setpoint temperature, and the slope is close to one at all three belt speeds, so an increase in the maximum setpoint temperature gave an approximately equal increase in the measured peak temperature. There is quite a bit of scatter in this graph, and the scatter seems to increase with the belt speed. However, the data seems to indicate that the maximum setpoint temperature has to be changed by approximately 15°C to reach the same peak temperature when the belt speed is increased by 50 cm/min.

Figure 3 shows the measured temperature profiles used to produce the best cell fired at each belt speed. Table 2 shows some characteristic measurements from these temperature profiles, and table 3 shows the results from these cells.

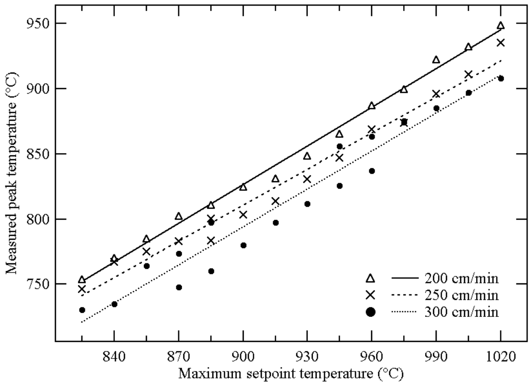

Figure 2: Measured peak temperatures at different maximum setpoint temperatures.

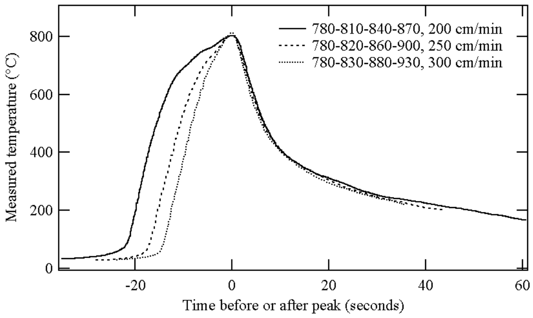

Figure 3: Measured temperature profiles used to produce the best cell fired at each belt speed.

It is seen from figure 1 and figure 3 that there are only small differences between the heating rates and cooling rates of the different temperature profiles. What differs between the profiles are the peak temperature reached during firing, and the time the samples are at a high temperature. The heating up to 600°C happens in the first heat zone, while most of the cooling occurs in a transition tunnel after the fourth heat zone in the furnace. This tunnel has a length of 5 inches, and thus even at 300 cm/min a wafer would spend 2.5 seconds in this tunnel. In most cases, the temperature was below 600°C before the wafers exited the transition tunnel.

3.2 Efficiency and fill factor

As shown in Figure 4, the efficiencies for cells fired at a belt speed of 200 cm/min reached a maximum for a setpoint temperature between 855°C and 885°C in the last heat zone. The best efficiency measured for cells fired at this belt speed was 15.3%. For lower temperatures, the efficiency dropped rapidly, and for higher temperatures, there is also an efficiency drop, but not so steep.

For a belt speed of 250 cm/min, the best efficiencies were achieved with the setpoint of the last heat zone between 885°C and 930°C. These settings gave a peak temperature between 785°C and 830°C, and a time above 620°C between 11.6 seconds and 12.7 seconds. In this temperature range, several cells had an efficiency between 15.4% and 15.5%, the best efficiencies measured in this work. Outside this processing window, the efficiencies went down, and also at this belt speed steeper towards lower temperatures than upwards.

The highest efficiencies for wafers fired at a belt speed of 300 cm/min are between 945°C and 975°C. The

Belt speed (cm/min)	Heating rate	Cooling rate	Peak temp	Time above 620°C
200	63°C/s	60°C/s	802°C	17.0 s
250	62°C/s	59°C/s	804°C	10.0 s
300	69°C/s	65°C/s	812°C	9.2 s

Table 2: The heating rate between 100°C and 600°C, the cooling rate between 775°C and 625°C, the peak temperature, and the time above 620°C for the temperature profiles shown in figure 3.

Belt speed (cm/min)	η	FF	J_{sc} (mA/cm^2)	V_{oc} (mV)	R_s (mΩ)	R_{sh} (Ω)
200	15.3%	77.7%	32.5	608	2.8	13
250	15.5%	76.9%	33.0	611	3.5	10
300	15.1%	75.8%	32.6	608	2.9	9.2

Table 3: Results from the best cell fired at each belt speed.

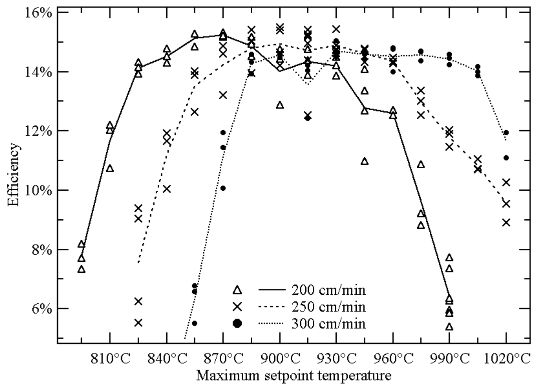

Figure 4: Measured efficiency at different maximum setpoint temperature. The lines show the average efficiency at each temperature.

best cell had an efficiency of 15.1%, and only one cell fired at a belt speed of 300 cm/min had an efficiency above 14.8%. The samples fired at 250 cm/min or 300 cm/min with low maximum setpoint temperatures had unstable contacts, and will be discussed in more detail in subsection 3.5.

The plots of efficiency vs maximum setpoint temperature for all the different belt speeds follow roughly the same shape, but are shifted along the temperature axis depending on the belt speed. The magnitude of this temperature shift seems to be about 30°C when the belt speed is altered by 50 cm/min. This difference in the setpoint temperatures is larger than what is necessary to get the same peak temperature in the temperature profile, so it seems like a combination of peak temperature and time at high temperature is needed to explain the variations in efficiencies.

The fill factor follows almost exactly the shape of the efficiency for the samples in this work, as can be seen in figure 5. Fill factors as high as 78% were achieved for a cell fired at 250 cm/min, while there were several cells fired at each belt speed that had a fill factor above 77%.

3.3 Short circuit current and open circuit voltage

The plot of the short circuit current in figure 6 has a temperature window between 885°C and 975°C where the current is approximately the same regardless of the belt speed used in the firing. At higher maximum setpoint temperatures, the short circuit current is reduced, and when the maximum setpoint temperature is below 885°C, the current quickly falls off according to belt speed.

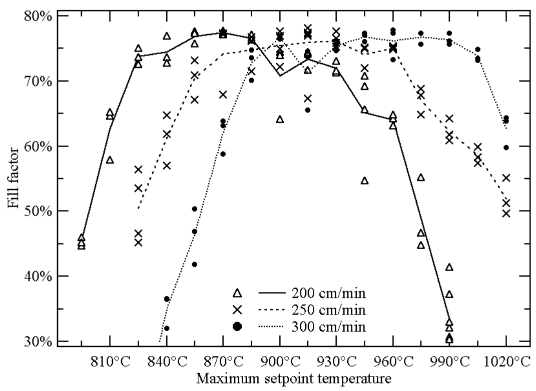

Figure 5: Measured fill factors at different maximum setpoint temperatures. The lines show the average fill factor at each temperature.

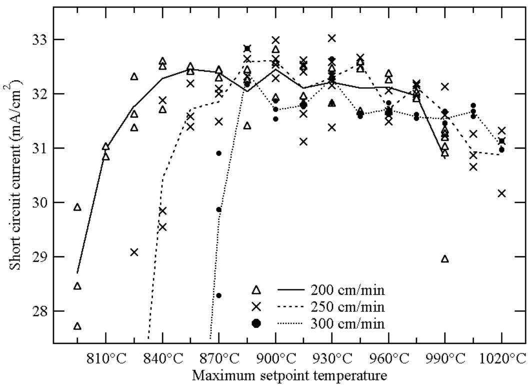

Figure 6: Measured short circuit current at different maximum setpoint temperatures. The lines show the average short circuit current at each temperature.

The best cells fired at 250 cm/min had slightly higher short circuit current than the rest of the samples, while the best short circuit current for cells fired at 300 cm/min is not as high as for cells fired at lower belt speed.

The open circuit voltage from all the samples in this work were between 587 mV and 612 mV, as shown in figure 7. For all belt speeds, the open circuit voltage was at a maximum close to 870°C, and when the maximum setpoint temperature was changed significantly from this value, the open circuit voltage was reduced. Again, the best cells fired at 250 cm/min were better than the rest of the samples, with the highest values of open circuit voltages. There are a lot of scatter in this plot, and no clear dependency between the open circuit voltage and the belt speed can be seen.

3.4 Series resistance and shunt resistance

As shown for all three belt speeds in figure 8, the series resistance has a minimum in the temperature range examined. For a belt speed of 200 cm/min, this minimum occurs at a maximum setpoint temperature between 840°C and 885°C. When the belt speed is 250 cm/min, the minimum is between 900°C and 930°C, while for a belt speed of 300 cm/min, the lowest series resistances are measured between 915°C and 945°C. The actual minimum values measured for series resistance are around 2 mΩ when the belt speed is 300 cm/min, and around 3 mΩ for lower belt speeds.

When the maximum setpoint temperature is increased above or reduced below the temperature with the minimum, the series resistance quickly increases. The

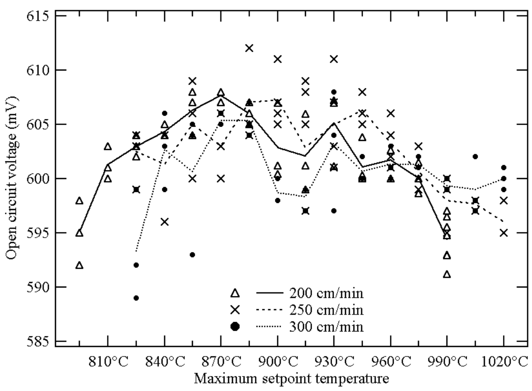

Figure 7: Measured open circuit voltages at different maximum setpoint temperatures. The lines show the average open circuit voltage at each temperature.

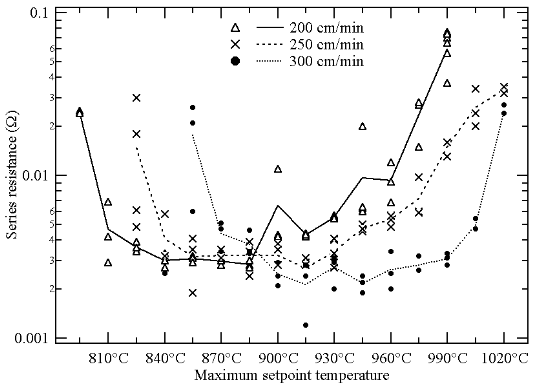

Figure 8: Measured series resistance at differennt maximum setpoint temperatures. The lines show the average series resistance at each temperature.

maximum values measured were about an order of magnitude larger than the minimum values, and again the graphs seems to have shifted by 30°C when the belt speed is increased by 50 cm/min. No series resistance values could be found for cells fired at 300 cm/min with a maximum setpoint temperature of 855°C or lower, as discussed in the next subsection.

There are a lot of scatter in the data for shunt resistance, as shown in figure 9, but still it can be seen for all belt speeds that when the maximum setpoint temperature was low, the shunt resistance was low, while higher maximum setpoint temperatures gave higher shunt resistance and less shunting of the solar cells.

It is not clear why low firing temperatures resulted in a low shunt resistance, but one probable explanation is that this simply was an artefact from the curve fitting. In this work, IVFIT was used to fit the two-diode model to the measured data, but this model might not be a good way to represent a solar cell fired at low temperature. For instance, simple circuit simulations have shown that a Schottky barrier diode in parallel with the series resistance would give an IV characteristic that appears to have low shunt resistance. Low temperature firing could easily give a Schottky barrier at the contact.

For cells fired at a belt speed of 200 cm/min, it can also be seen that a maximum setpoint temperature above 960°C gave low shunt resistance. This probably means that the front grid has been fired all the way through the emitter of the solar cells, at least in some points. At the highest setpoint temperature used with a belt speed of 250 cm/min, it may seems like the shunt resistance is beginning to go down, but the value of the shunt resistance is still acceptable. For the highest belt speed of 300 cm/min the shunt resistance of the fired cells does not go down even at a setpoint of 1020°C in the last zone, so even at this temperature the contacts are not fired through the emitter of the solar cells.

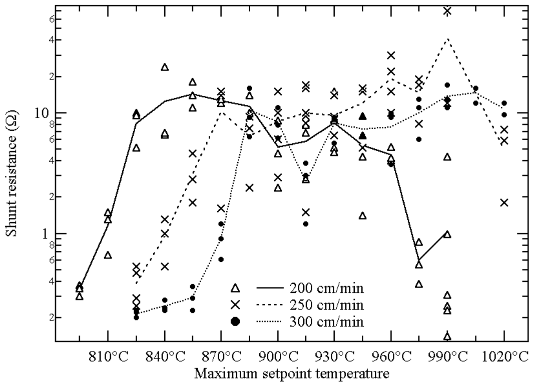

Figure 9: Measured shunt resistance at different maximum setpoint temperatures. The lines show the average shunt resistance at each temperature.

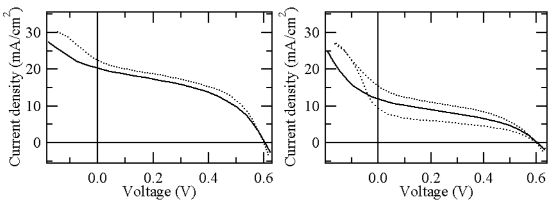

Figure 10: IV curves measured for cells fired at (left) 250 cm/min with a maximum setpoint temperature of 825°C, and (right) 300 cm/min with a maximum setpoint temperature of 840°C.

3.5 Unstable contacts

For cells fired at 300 cm/min with a maximum setpoint temperature at 855°C or lower, and cells fired at 250 cm/min with a maximum setpoint temperature of 825°C, the IV curves had a strange shape, as seen on figure 10. These curves could not be fitted to the normal two-diode IV function, and thus are the characteristic parameters extracted by IVFIT for these samples dubious.

These cells did not have constant IV characteristics either, but instead a different IV curve was measured with each measurement. First after several measurements on the same sample, would the IV curve stabilize. This was taken as an indication that the firing process for these cells was incomplete, and that the heat generated from the current going through the contacts during the measurement actually continued the contact formation. The IV curves were measured from positive to negative voltages. The stabilized IV curves still had very high series resistance, and the fill factor of the stabilized IV curve did never exceed 25%.

3.6 Contact resistance mapping

Corescan was extensively used to analyse the fired cells. Examples of such Corescan plots can be seen in figure 11 and figure 12. The cell shown in figure 11 was a cell with low value of series resistance. On such cells,

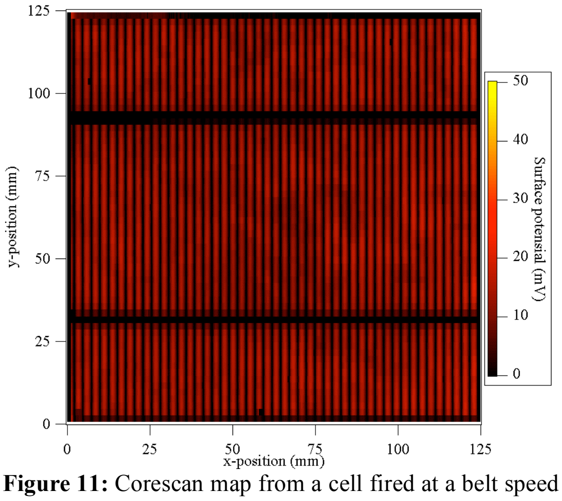

Figure 11: Corescan map from a cell fired at a belt speed of 250 cm/min with a maximum setpoint temperature of 915°C. This cell has insignificant contact resistance.

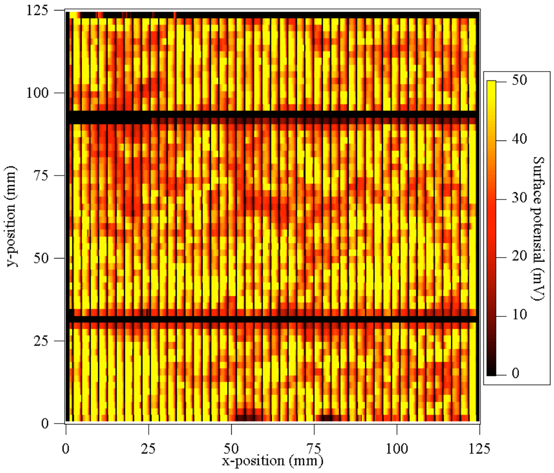

Figure 12: Corescan map from a cell fired at a belt speed of 250 cm/min with a maximum setpoint temperature of 1005°C. This cell has large values of contact resistance.

as can be seen from the plot, most of the surface has a really low surface potensial when the cell is short circuited, with no or few areas of higher voltage. This shows that there are low series resistance losses in the solar cell.

Cells fired at higher temperatures had both higher voltage values in average, and larger spread of different voltages over the surface. This shows that there are large losses due to series resistance in the solar cell, and also that different parts of the cells will be operating at different voltage, thus giving fill factor losses due to a more rounded IV curve.

In figure 13, one scan line from the center between the two busbars in both figure 11 and figure 12 have been ploted. Each of these scan lines are typical for one or the other plot, and they show both the difference in homogenity between the two plots, and the higher average values on the scan line from figure 12. As can be seen in the plot, the parabolas at the top of each peak for the most cases look the same between the two cells, and also the minimum values from both graphs go all the way to zero. This means that the two cells have the same emitter sheet resistance, and that there are small losses in the front grid.

The parabolas on the scan line for the cell fired at high temperature are offset with a voltage difference, and this shows that the increased series resistance losses are due to high contact resistance at the metal-silicon interface. This is believed to be caused by a thick glass layer beneath the contacts, as is often seen when firing contacts at high temperature [3].

4 CONCLUSION

Different temperature profiles have systematically been examined to find the optimum firing conditions for a RTC LA-309 firing furnace with four heat zones and water cooling. The belt speed and setpoint temperature in the different heat zones were used to change the temperature profile. The best results were achieved at a belt speed of 250 cm/min with a maximum setpoint temperature between 885°C and 930°C. With these parameters, several cells had an efficiency between 15.4% and 15.5%, and a fill factor between 77% and 78%. These cells had uniform contacts with low series resistance and relatively high shunt resistance.

Cells fired at high belt speeds with low temperatures were not throughoutly fired, and had IV characteristics that changed with each measurement. Only after several measurements would the IV characteristics stabilize. On the other hand, cells fired at high temperature and slow belt speeds got higher series resistance. Analysis with Corescan showed that this was due to increased contact resistance.

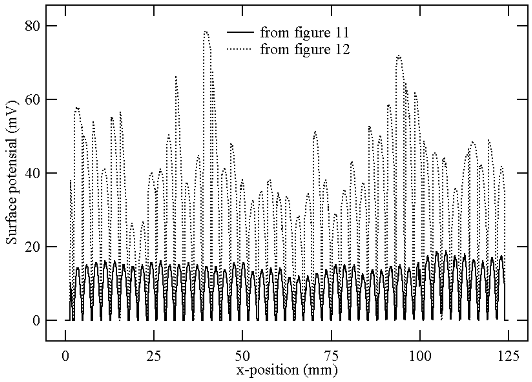

Figure 13: Plot of one scan line from the cells in figure 11 and figure 12. The scan lines are from the middle of the cells, between the two busbars.

5 ACKNOWLEDGEMENT

This work has been funded by the Nordic Energy Research through the scientific project “Solar Electricity, from Materials to System Integration (Nordic PV)”.

6 REFERENCES

[1] http://www.ecn.nl/en/zon/products-services/i-v-curve-fitting-program-ivfit/

[2] A.S.H. van der Heide et al., Proceedings 29th IEEE Photovoltaic Specialists Conference, (2002), 340.

[3] C. Khadilkar et al., Proceedings 20th European Photovoltaic Solar Energy Conference, (2005), 1291.